J. Embryol. exp. Morph. 93, 267–280 (1986)
Printed in Great Britain © The Company of Biologists Limited 1986

Clonal analysis of chimaeric patterns in aortic endothelium

GÜNTER H. SCHMIDT*, MAUREEN M. WILKINSON AND BRUCE A. J. PONDER

Institute of Cancer Research, Haddow Laboratories, Clifton Avenue, Sutton, Surrey SM2 5PX, UK

SUMMARY

The mosaicism in aortic endothelium of mouse aggregation chimaeras is demonstrated using the lectin *Dolichos biflorus* agglutinin as a strain-specific marker. The general fragmentary appearance and considerable size range of patches suggests that endothelial cells do not proliferate in a highly coherent manner. The developmental significance of the observed patterns is investigated by means of a quantitative statistical analysis – the Greig-Smith analysis of variance. This method examines the spatial distribution of patches and is able to detect and characterize pattern at various scales. The results show that (1) patches are non-randomly distributed at all scales examined and (2) 'clusters of clusters' occur at one small and one large scale, defining territories of 'primary' and 'secondary' descendent clones, which arose respectively during early and late periods in the development of the endothelium. We conclude from this analysis that (1) cell mixing is never complete, even in the early embryo and (2) cell mingling is not uniform during development. A different pattern was previously demonstrated for intestinal epithelium (Schmidt, Wilkinson & Ponder, 1985*c*) indicating the potential value of the method for quantitative comparison of mosaicism between tissues and also different developmental stages. Our results suggest that the analysis of patch sizes is likely to be less informative in terms of developmental mechanisms, than the analysis of the spatial arrangement of patches.

INTRODUCTION

A carbohydrate-based polymorphism recognized by the lectin *Dolichos biflorus* agglutinin (DBA) provides a histochemical marker of chimaerism between inbred mouse strains (Ponder, Festing & Wilkinson, 1985*a*). The polymorphism is confined to intestinal epithelium and vascular endothelium. We have used the DBA marker system for studying clonal development of crypts of Lieberkühn, and for visualizing cell migration pathways in the intestinal epithelium of aggregation chimaeras (Schmidt, Wilkinson & Ponder, 1984, 1985*b,c*; Ponder *et al.* 1985*b*; Schmidt, Garbutt, Wilkinson & Ponder, 1985*a*). Here, we report the results of the application of the DBA marker to the quantitative clonal analysis of aortic endothelium.

* Present address: Frauenhofer-Institut für Toxikologie und Aerosolforschung, Stadtfelddamm 35, 3000 Hannover 61, FRG.

Key words: mouse, chimaera, aortic endothelium, clonal analysis, *Dolichos biflorus* agglutinin.

The aorta is formed *in situ* from 'blood islands' – clusters of cells developing in the splanchnic mesoderm. Cells in the peripheral zone of blood islands flatten to become the endothelium, a special type of epithelium, while cells in the central zone become primitive blood corpuscles (Jenkinson, 1925). Adjacent blood islands coalesce to form tubes. During subsequent development the paired dorsal aortas, which run along both sides of the notochord, fuse to form a single descending aorta and eventually acquire outer walls of connective tissue. The endothelium, separated from the surrounding outer layers by basal lamina, lines the aorta as a monolayer of exceedingly thin cells which are greatly elongated in the long axis (Thorgeirsson & Robertson, 1978).

In the adult, endothelial cells retain a capacity for cell division and movement: spreading, migration and subsequent proliferation of endothelial cells occurs at the sites of mechanical injuries or lesions (Hauenschild, 1980). Cell turnover in the normal adult endothelium is relatively slow: on average, 0·3–1·5 cells in a hundred are replaced per day in the rat aorta. Marked regional heterogeneities in [^{3}H]thymidine uptake exist however, and it was suggested that heavily labelled regions might represent growth centres, comparable to intestinal crypts, from which outward migration of cells occurs (Schwartz & Benditt, 1973). Our chimaeric system would reveal any highly ordered arrangement of proliferative compartments and of cell migration pathways such as occur in the intestinal epithelium (Ponder *et al.* 1985*b*; Schmidt *et al.* 1985*b*).

The primary objective of the present study was to define a clonal pattern characteristic of the aortic endothelium, and thereby to gain insight into the clonal history of the development of the endothelium using the quantitative methods of clonal analyses developed by us (Schmidt *et al.* 1985*a,c*). Two types of clones are distinguished in the analysis. A 'coherent clone' is a group of cells which are descended from a common progenitor cell through previous divisions and which have stayed together as a coherent group. A 'descendent clone', by contrast, is a group of cells related by descent from a common progenitor, but which may have separated by cell mixing and are therefore no longer contiguous. In chimaeras with balanced proportions of components, individual clones may be obscured by aggregation into larger patches, but in chimaeras with unbalanced proportions, each patch may be regarded as a single coherent clone (West, 1975; Whitten, 1978), and clusters of patches may be recognized, which can be interpreted as single descendent clones (Schmidt *et al.* 1985*c*).

MATERIALS AND METHODS

Animals

Three DDK ↔ C57BL/6JLac (B6) and one RIII-*ro* (RIII) ↔ B6 mouse aggregation chimaera were constructed at the MRC Laboratories, Carshalton, according to methods described by Mintz (1971*a*). The ages of the mice and the relative proportions of the parental components (for method see below) are given in Table 1. In order to minimize the effect of patch aggregation (see Schmidt *et al.* 1985*a,c* for discussion), we restricted our analysis to mice with highly unbalanced

proportions. The aortas chosen were the most unbalanced out of 25 chimaeric preparations examined.

Preparations

Animals were killed by ether overdose. Large segments of thoracic aortas (cf. Table 6) were dissected from the chimaeras, transferred to wax-based Petri dishes containing PBS, cleared of adventitious loose connective tissue and fat, and cut open dorsally (using dissecting scissors, Prof. Kinmoth's Scissors, Macarthy's Surgical Ltd, Dagenham, Essex, and forceps, Micro-Surgery, Serr. 4″, Macarthy's Surgical Ltd). Any remaining blood was removed by gentle pipetting. The preparations were pinned out and slightly stretched to approximately the *in situ* length. They were then fixed and stored in 10% formol saline.

Staining

Aortic endothelia were stained with *Dolichos biflorus* agglutinin (DBA)–peroxidase conjugate. The conjugates were prepared by the periodate method (for details see Ponder & Wilkinson, 1983).

Following fixation the preparations were incubated for 30 min in 0·1% phenylhydrazine HCl in PBS pH 7·3 to block endogenous peroxidase, washed in PBS, transferred to PBS containing 0·5% bovine serum albumin (PBS–BSA) (30 min), and incubated overnight in DBA–peroxidase conjugate 1:75 in PBS–BSA. The peroxidase was subsequently demonstrated using 3′3′ diaminobenzidine (DAB) as a substrate yielding a brown reaction product (10 mg DBA (Sigma) + 20 ml 0·1 M-Tris buffer, pH 7·3 + 40 μl 30% H_2O_2). Following incubation for 5 min, preparations were washed in PBS. To ensure that the endothelial layers were undamaged, cell nuclei were stained with Mayer's haemalum (3 min), after preparations had been scored and photographed (see below).

Analysis of patch size

DBA serves as a strain-specific marker because endothelial cells of DDK or RIII but not B6 origin express DBA-binding sites (Ponder & Wilkinson, 1983; Ponder *et al.* 1985*a*).

Numbers of DDK (chimaeras 45,46) or RIII (chimaera 49) cells per patch were counted (patch size). Chimaera 47 was not analysed as the DBA-negative (i.e. unstained) cells of the B6 minority component could not be counted following our protocol. Enumeration of the numbers of DBA-positive cells was possible as areas containing cell nuclei appeared lighter than the surrounding stained cytoplasm. Scoring was carried out before counterstaining with Mayer's haemalum (see above) which unavoidably also stained the nuclei in the relatively thick intimal layers underlying the endothelium.

Using the method of maximum likelihood, geometric distributions were fitted to the observed patch-size-frequency data and tested for goodness of fit by means of χ^2-tests (Ross, 1980).

The percentage contribution of the minority component (Table 1) was calculated by the line interception method (Aherne & Dunhill, 1982). The entire preparation was scanned under ×80 magnification (10/0·25 objectives; Leitz Laborlux 12, Wetzlar) and the number of interceptions of a 10×10 eyepiece graticule overlying cells of the minority component was scored. This number, divided by the total number of points sampled (400–500 for each aorta), ×100, yielded an estimate of the percentage of the minority component.

Spatial analysis: the Greig-Smith analysis of variance

The method, which is an exploratory statistical technique (Greig-Smith, 1983), has been described in detail elsewhere (Schmidt *et al.* 1985*c*). The principle of the analysis is to examine the distribution of numbers of objects (in the present case, mosaic patches) scored by means of a grid. If the objects are randomly distributed the numbers of objects per square of the grid will conform to a Poisson distribution (see below); if they are clustered or regularly spaced, the distribution will depart from this expectation. By repeating the analysis for larger blocks obtained by combining adjacent grid squares, the occurrence of pattern at different scales can be sought (cf. Fig. 5).

The mathematical analysis is based on the analysis of variance (ANOVA). This analysis is performed for *each* block size. The ANOVA establishes the variability in the numbers of patches found between the sample blocks at a particular block size. In the Greig-Smith method the ANOVA does not, however, involve computation of the components of variance in the usual sense (cf. Bailey, 1978); instead, mean square/mean ratios (Index of Distribution [IOD]) are calculated separately for each block size as described in Schmidt *et al.* (1985*c*; Table 1). A set of IODs obtained from replicate tissue samples should conform to a χ^2-distribution if patches are randomly (Poisson) distributed. IOD values lower than expected indicate regular spacing, while higher IODs indicate clustering. A distinction between x- and y-directions can be made, allowing one to test for differences of pattern in the longitudinal and transverse directions.

Evidence of pattern is sought as follows: IOD ratios of successive block sizes are expected to fluctuate around 1, the expected range depending on the degrees of freedom at the particular block size (Table 4). If IODs for one block size are *consistently* larger than the IODs for the immediately smaller block size, the IOD ratios will be consistently larger than 1 and, in addition, some values may be significantly high. In that case, clustering or, if an overall non-random distribution has already been established, an increase in the intensity of pattern may be inferred at about the order of the larger block size. While the initial search for consistent increases of IODs in the data involves a subjective assessment (Table 2), the validity of that interpretation is subsequently tested using the F-statistic (Table 4).

The positions of discrete patches of the minority component on photomontages of the aortas were mapped by recording the coordinates of patch centres (judged visually) with the aid of a digitizing tablet (MOP Videoplan, Kontron). The thoracic aortas were divided into proximal and distal halves, except for aorta 46 for which only a short region of midthoracic aorta was obtained. A 'form factor' (cell length/width = 3·32) was used to correct for the longitudinal shapes of cells. This was determined using a MOP Videoplan, on 50 randomly chosen endothelial cells (random number tables, Lindley & Scott, 1984: cells were identified by nuclear staining with Meyer's haemalum, and outlines of cell bodies were visualized as dark-brown lines by treatment with 0·2% silver nitrate and subsequent exposure to light (Pool, Sanders & Florey, 1958)). A 16×16 grid was used in the mathematical analysis, which yielded a mean number of approximately one patch per quadrat (Fig. 5; Schmidt *et al.* 1985*c* for further explanation).

Photography

Aortas were photographed on a Leitz Orthoplan microscope with a plate camera attachment using Ilford FP4, 4″×5″, 125 ASA film.

RESULTS

(A) *Patch sizes*

Examples of the general appearance of patches are given in Figs 1 and 2. Patches were often conspicuously longitudinally arranged, i.e. in the direction of the blood

Table 1. *Sources from which aortas were obtained, and percentage contributions of component strains*

Chimaera number	Strain combination	Age (weeks)	Percentage of minority component*
45	DDK↔B6	12	3·0 (DDK)
46	DDK↔B6	9	5·5 (DDK)
47	DDK↔B6	17	8·5 (B6)
49	RIII↔B6	21	6·1 (RIII)

* DDK, RIII, endothelium positive; B6, endothelium negative (i.e. unstained).

flow, but the longitudinal shape of endothelial cells (cf. Materials and Methods) will have exaggerated the shape of patches. Indeed, when the elongated cell shape was corrected for in the Greig-Smith analysis (see Materials and Methods) no consistent difference between the x- and y-directions over all seven samples were found, which implies that the longitudinal appearance of patches may be a visual deception. IOD values were averaged (Table 2) when splits in the x- and y-directions were performed (at block sizes 2, 8 and 128 – cf. Schmidt *et al.* 1985*c*).

The fragmentary nature of the patches was reflected in the patch-size-frequency distributions which revealed a preponderance of singletons. The overall concave shapes of the distributions fitted a geometric model (Fig. 3).

(B) *Spatial distribution of patches*

The analysis revealed an overall non-random distribution of patches as 53 out of 56 IOD values were greater than 1 (Table 2). This conclusion was validated by comparing the IODs with the χ^2-distribution for each of the eight scales examined (Table 3).

In order to detect an increase of clustering at a particular scale it was necessary to identify consistencies of increases of IODs. Subjective assessment of the values given in Table 2 suggested two such increases: one at block size 2, and a further one at block size 32. An objective assessment of the strength of the evidence for our conclusion was provided by using the F-statistic. The ratios of successive IODs were determined and compared with the F-distribution by examining complete sets of replicate samples (similar to the χ^2-procedure, cf. Table 3). The results (Table 4) indicate that a definite increase in the strength of pattern occurred at block size 2, as all F-values at the 2:1 level of comparison were above 1 and, moreover, three of them were significant. A further increase is probable at block size 32, as six out of seven IOD ratios at 32:8 were above 1; one of them was significant. There were no consistent trends at other block sizes as successive IOD ratios were fairly evenly spread above and below 1. The lack of further change in pattern justifies combining block sizes 2 to 16, and 32 to 128 for a summarizing graphical representation (Fig. 4). The F-test of the summarized data (Table 5) presents strong evidence for a strengthening in the pattern at block sizes 2 and 32.

Having demonstrated a non-random arrangement of patches (Tables 2, 3) and having detected two scales at which clustering of patches occurred, we proceeded to identify the pattern in the preparations of aortic endothelium. An example of this procedure is given in Fig. 5. It is reasonable to suggest that the patches which clustered at block size 2 were related by origin from a single source, representing 'descendent clones' of DDK cells; further clustering at the larger block size 32 was thus indicative of a further level of 'descendent clones'. On the basis of this hypothesis we were able to calculate the total numbers of large-scale descendent clones for each preparation of thoracic aortic endothelium (Table 6). An interpretation of the different scales of clustering in terms of clonal development is given below.

Fig. imaeric pattern in DDK↔B6 aortic endothelium (chimaera 45) stained with *Dolichos biflorus* agglutinin (DBA)–peroxi conjugate. Only DDK cells (stained) express DBA-binding sites. The relatively fine grain size of the mosaic pattern and fragm y appearance of patches (*p*) are apparent. The slight curvature in some of the aggregates of patches is due to contraction of elasti ue in the aortic wall. The longitudinal appearance of the patches is due to the elongated shape of the endothelial cells. Arrov icates single cell patch in an area shown at higher magnification in Fig. 2. *a*, opening of intercostal artery; *p*, patches of DDK . Bar, 1 mm.

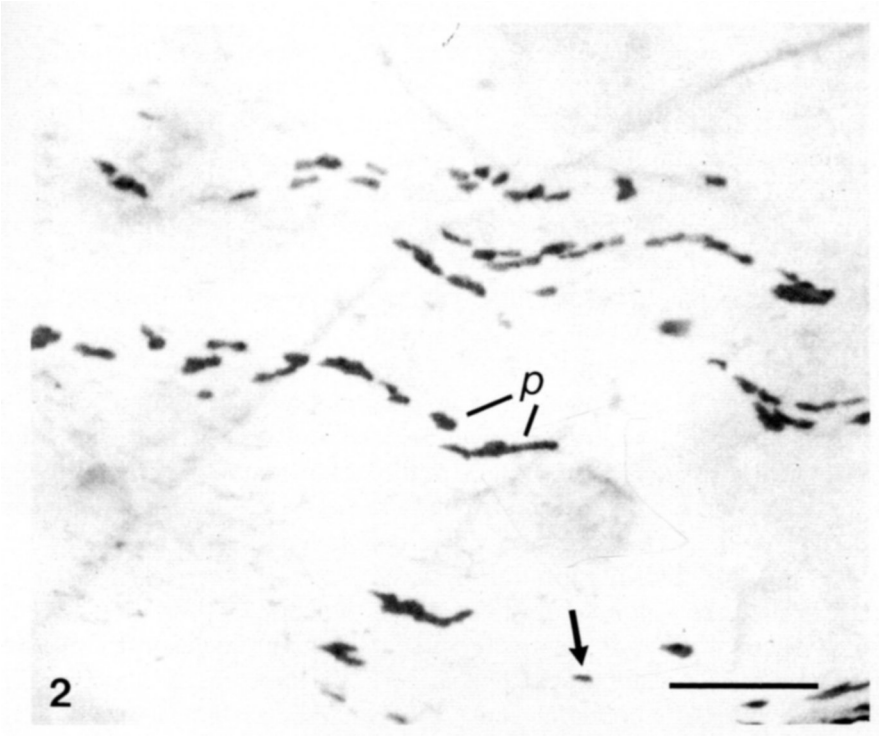

Fig. 2. High magnification of part of DDK↔B6 aortic endothelium shown in Fig. 1. Arrow indicates the same single cell patch in both Figs. *p*, patches of DDK cells. For further explanation see legend to Fig. 1. Bar, 200 μm.

Table 2. *Index of distribution (IOD) values obtained from the Greig-Smith analysis of variance*

		Block size (d.f.)							
Sample number	Chimaera number	1 (64)	2 (128)	4 (16)	8 (32)	16 (4)	32 (8)	64 (1)	128 (2)
1	49	1·61	1·97	2·91	2·27	0·83	4·07	18·52	5·34
2	49	1·28	1·60	1·40	1·69	4·06	9·11	15·51	13·26
3	47	1·17	1·65	1·40	1·84	1·76	2·66	1·94	13·28
4	47	1·12	1·58	1·65	2·69	4·51	2·28	8·75	20·71
5	45	1·11	1·98	2·48	4·47	2·96	4·92	0·34	11·33
6	45	1·20	1·52	3·11	2·57	2·68	4·72	0·77	7·89
7	46	1·10	2·14	1·20	2·01	1·32	11·23	1·78	5·69

IODs are consistently greater than 1, indicating that patches were non-randomly distributed. This conclusion was validated by comparing IODs with the χ^2-distribution (Table 3). Subjective assessment suggests that there was no change in pattern for block sizes enclosed in brackets, but stronger clustering occurred at block sizes 2 and 32. This conclusion is confirmed by examining the IOD ratios using the F-statistics (Table 4).

DISCUSSION

The two levels of clonal pattern are difficult to interpret on the basis of well-defined growth centres and outward directions of cell migration in the adult tissue such as might be inferred from the findings of Schwartz & Benditt (1973) (see Introduction). Cell turnover in normal adult aortic endothelium is low and it seems probable that the patterns which we observe reflect overwhelmingly the effects of cell proliferation and mingling during the growth and development of the tissue.

Large-scale (primary) descendent clones included several small-scale (secondary) descendent clones which would be expected if the former were older in developmental terms than the latter. It is therefore reasonable to argue that the small-scale spatial pattern arose late in development but that the large-scale pattern arose during a relatively longer period, and reflects events which took place during early tissue growth. Fragmentation of primary descendent clones into spatially identifiable groups of discrete coherent clones may have resulted from the continued incursion of cells of the other component into primary descendent clones as a result of cell division during tissue growth. There is evidence that in the adult in at least some circumstances (e.g. wounding), endothelial cells can migrate. Cell migration, if relatively restricted, may have contributed to the fragmentation of secondary descendent clones. This interpretation implies that (1) growth is not primarily coherent and (2) cell mingling is not a uniform process throughout development. Furthermore, the finding of non-randomness at all scales suggest that (3) mixing is never complete, even in the early embryo. This

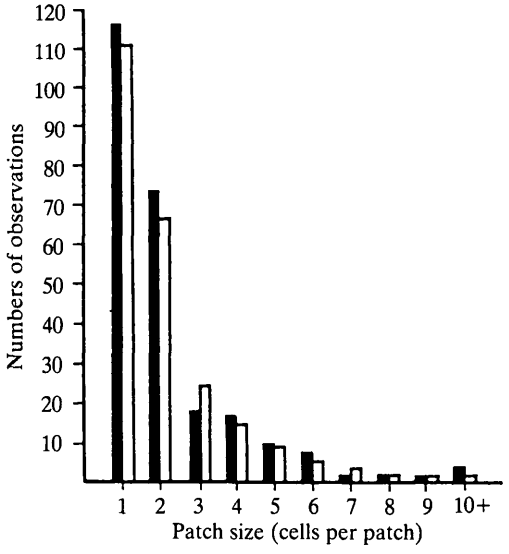

Fig. 3. Chimaera 45. Size frequency distribution of patches of DDK cells. The observed distribution (solid bars) fitted a geometric distribution (open bars), calculated from the observed data. χ^2-value: 8·2 on 9 d.f. (not significant, $P > 0{\cdot}05$). The two other aortas tested (see Materials and Methods) yielded similar results.

conclusion is consistent with observations that some coherent growth occurs already at the pre-implantation stage (Gardner, 1984*a*), although there may be exceptions for a few tissues (McLaren, 1976; Mullen, 1977: Gardner, 1984*b*).

Using block size 32 as a guide, we were able to define the approximate outlines or territories, and hence also the total numbers, of primary descendent clones. We assume that each descendent clone occupies a territory of roughly similar size: they would not otherwise have been detected by our analysis. (Note that this does not imply that each must also comprise a similar number of cells: Fig. 1 shows that in this respect descendent clones may be highly variable, as we would have predicted from our previous studies of coherent clone sizes in chimaeric tissues (Schmidt *et al.* 1985*c*).) Our data (Table 6) indicate that there are of the order of 5–20 descendent clones per mm^2 in the endothelium of the thoracic aorta. This figure reflects the number of patches present at the end of a phase of extensive (but not necessarily complete) mingling which must be presumed to have occurred early in the development of the endothelium. It does not tell us about the number of cells originally allocated, some or all of whose descendents would contribute to the endothelium.

Table 3. *Comparison of IOD values with the χ^2-distribution*

Expected numbers	1·75	Lower quartile <(75%)>	1·75	Median <(50%)>	1·75	Upper quartile <(25%)>	1·75
1 d.f.		<0·10>		<0·45>		<1·32>	
Observed numbers	0		1		1		5
2 d.f.		<0·29>		<0·69>		<1·39>	
	0		0		0		7
4 d.f.		<0·48>		<0·84>		<1·35>	
	0		1		1		5
8 d.f.		<0·63>		<0·92>		<1·28>	
	0		0		0		7
16 d.f.		<0·74>		<0·96>		<1·23>	
	0		0		1		6
32 d.f.		<0·82>		<0·98>		<1·16>	
	0		0		0		7
64 d.f.		<0·86>		<0·99>		<1·11>	
	0		0		1		6
128 d.f.		<0·91>		<0·99>		<1·08>	
	0		0		0		7

If the IOD values from the 7 samples conformed to the χ^2 distribution, on average 1·75 samples would lie in each of the quartiles (top row of table: expected numbers). In fact, the observed values are heavily weighted towards the upper quartile, indicating a non-random distribution of patches with clustering.

The 75%, 50% and 25% points of the χ^2-distributions were obtained from statistical tables (Lindley & Scott, 1984; the values not given in the tables were obtained through the computer algorithm supplied by NAG (Numerical Algorithms Group Ltd, Oxford) by finding the value for the particular degrees of freedom, and dividing that figure by the d.f., e.g. 75% point for 128 d.f. is 116·88, divided by 128 equals 0·91 (bottom row, lower quartile).

A different spatial pattern with only one scale of descendent clones was found in the clonal analysis of intestinal epithelium (Schmidt *et al.* 1985*c*), which suggests that this exploratory statistical method of analysis is able to define a clonal pattern characteristic for a particular tissue. It may therefore provide a quantitative basis for comparison between mosaic patterns found at different developmental stages, and may also be of value in assessing the results of experimental manipulation of tissue development, and possibly the validity of computer models of tissue growth. The analysis was carried out for tissues in which the spatial position and numbers of coherent clones could be confidently inferred from that of observed patches in unbalanced, two-dimensional preparations of epithelia. However, the method should still be able to define a tissue-specific pattern even if discrete patches (and therefore also numbers of descendent clones) cannot be defined, as would be the case if the components of the chimaeras were more nearly balanced. In that case, percent cover per quadrat rather than discrete patches would have to be scored (Greig-Smith, 1983; see also Schmidt *et al.* 1985*c*).

Table 4. *Testing for scale of pattern by examination of successive IOD ratios using the F-statistic*

Sample number	Chimaera number							
		↓				↓		
1	49	1·22	1·48	0·78	0·37	4·90	4·55	0·29
2	49	1·25	0·88	0·88	2·40	2·24	1·70	0·85
3	47	1·41*	0·85	1·31	0·96	1·51	0·73	6·85
4	47	1·41*	1·04	1·63	1·68	0·50	3·84	2·37
5	45	1·78*	1·25	1·80	0·66	1·66	0·07	33·32
6	45	1·27	2·05*	0·83	1·04	1·76	0·16	10·25
7	46	1·34	0·56	1·68	0·66	8·50*	0·16	3·20
Level of comparison (Block sizes)		2:1	4:2	8:4	16:8	32:16	64:32	128:64
Value significant if above –		1·37	1·64	2·18	2·67	6·04	5·32	199·5
(d.f.)		(128,64)	(16,128)	(32,16)	(4,32)	(8,4)	(1,8)	(2,1)
Value significant if below –		0·77	0·50	0·50	0·17	0·26	0·004	0·05
(d.f.)		(64,128)	(128,16)	(16,32)	(32,4)	(4,8)	(8,1)	(1,2)

Observed IOD ratios are expected to fluctuate around 1 if there is no change in pattern (similar to the χ^2-expectation, cf. Table 2). Significant departures from the expected distribution are determined by use of the F-statistic. (Note the varying degrees of freedom (d.f.) and therefore varying significance values of the F-distribution.) An increase in the *strength* of pattern is identified when IOD ratios are consistently greater than 1, and some values are significant at the 5% level (these are marked with an asterisk *; note that even though one ratio at 4:2 was significant, only 4/7 ratios were actually greater than 1, i.e. values fluctuated around 1 indicating no change in pattern). No values were significantly low, which would have indicated a decrease in pattern. The data suggest that clusters occurred at scale 2, and clusters of clusters at scale 32 (arrows).

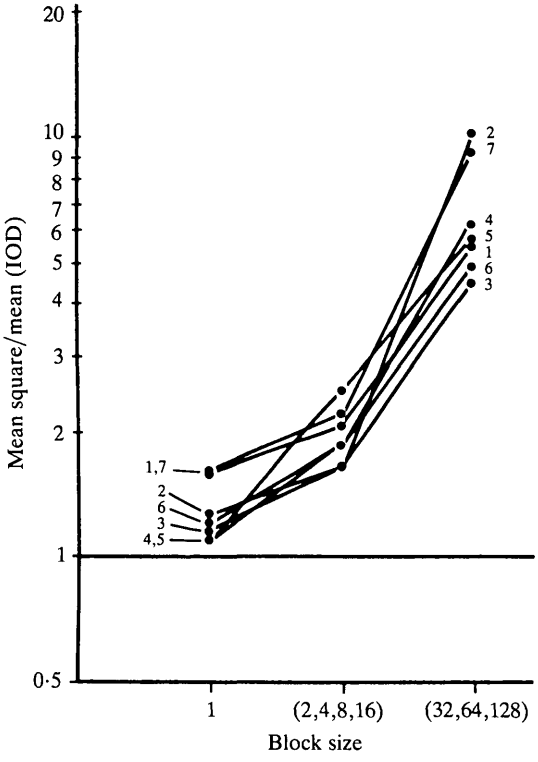

Fig. 4. Demonstration of increase in pattern at two scales. By testing successive IODs for each of the seven replicas (Tables 4, 5) we were able to show consistent increases of pattern at block sizes 2 and 32, and to combine block sizes 2, 4, 8, 16, and 32, 64, 128 (see text for further explanation). The IODs at these scales are shown for each sample: the numbers on the graph refer to the sample numbers in Tables 1–4.

Table 5. *Successive IOD ratios for combined block sizes*

Sample number	Block size	
	(2,4,8,16):1	(32,64,128):(2,4,8,16)
1	1·29	2·69*
2	1·29	6·33*
3	1·42*	2·73*
4	1·65*	3·36*
5	2·24*	2·28*
6	1·56*	2·64*
7	1·26	4·63*
Values significant if above –	1·37	1·79
(d.f.)	(180/64)	(11/180)

The F-statistic confirms the increases in the strength of pattern at scale 2 and 32 (for further explanation, see legend to Table 4).

Although the establishment of patch-size-frequency distributions and subsequent comparison of the distributions with theoretical models (here, geometric) have allowed us to test the validity of previous statistical methods for estimation of

Fig. 5. *Top*: 16×16 grid which was used in the Greig-Smith analysis of variance. The grid shown is elongated to allow for the endothelial cell shape. Heavy lines on the left show block size 32, on the right block size 2. There were no consistent differences in the extent of clustering detected whether the block was orientated in x-direction (lower rectangle) or y-direction (upper rectangle) and IOD values obtained from x- and y-splits were therefore averaged (see text). *Bottom*: Chimaera 45. Diagrammatic drawing of Fig. 1 showing spatial arrangement of DDK patches, and how the results from the mathematical analysis (see text) were interpreted: we regard the clustering identified at block sizes 32 and 2 as territories of 'primary' and 'secondary descendent clones'. Using block size 32 (top) as a guide we were able to identify the probable territories of five primary descendent clones. Three further putative territories appear incomplete as the sample area shown includes only part of the thoracic aorta. Each primary descendent clone contains several smaller, secondary descendent clones (territories indicated as an example in the primary descendent clone at the top right).

Table 6. *Numbers of large-scale descendent clones identified by the method outlined in Fig. 5*

Chimaera number	Percentage of minority component	Area examined (mm^2)	Observed numbers of descendent clones of the minority component	Calculated total numbers for either genotype	Clones mm^2
45	3·0	42·9	10	333	7·8
46	5·5	12·2	12	218	17·9
47	8·5	48·9	25	294	6·0
49	6·1	35·6	21	344	9·7

Total numbers were obtained by dividing the numbers of descendent clones scored by the relative proportion of the respective minority component. Measurements of areas were determined using a MOP Videoplan.

clone size in mosaic tissues (Schmidt *et al.* 1985*a*, 1986), such distributions may arise in a variety of ways (e.g. Ross, 1980) and are therefore of limited value in identifying the mechanisms of pattern formation (Schmidt *et al.* 1986). Here, good fit to geometric (which is in contrast to our previous results for intestinal epithelium) would be consistent with a random spacing of patch-progenitor cells (cf. Schmidt *et al.* 1985*a*), but the mathematical analysis of the spatial pattern clearly demonstrated an overall non-random arrangement of patches. The satisfactory description of the data by a geometric model may therefore be due to small scale, local fragmentation of larger patches (see above). The relatively fine grain of mosaic pattern due to overall small-patch sizes, and the fragmentary appearance of patches, implies that for the most part clones do not show coherent growth. Similar patchiness has now been reported by us for tissues derived from endoderm (intestinal epithelium), neuroectoderm (retinal pigment epithelium) and mesoderm (endothelium), which strongly suggests that this mode of tissue growth applies to mammalian epithelia in general.

Lewis, Summerbell & Wolpert (1972) questioned a claim made by Mintz (1971*b*) that the pattern of mosaic patches identified in chimaeric tissues may be of general developmental significance. We support Mintz's view and have shown that the use of appropriate mathematical methods in the analysis of mosaic patches in chimaeric epithelia may provide a general method to gain insight into clonal histories during tissue development. Our results suggest that the analysis of patch sizes is likely to be less informative than the analysis of the spatial arrangement of patches.

We thank Professor R. Mead for valuable discussions and advice with the statistical analysis and Mr D. J. Garbutt for carrying out the computer programming. This study was carried out during the tenure by B.A.J.P. of a Career Development Award from the Cancer Research Campaign, and was supported by a programme grant from the Medical Research Council and the Cancer Research Campaign.

REFERENCES

AHERNE, W. A. & DUNHILL, M. S. (1982). *Morphometry*. London: Arnold.

BAILEY, N. T. J. (1982). *Statistical Methods in Biology*. London: Hodder and Stoughton.

GARDNER, R. L. (1984*a*). Mammalian chimaeras – future perspectives. In *Chimaeras in Developmental Biology* (ed. N. Le Douarin & A. McLaren), pp. 431–443. London: Academic Press.

GARDNER, R. L. (1984*b*). An *in situ* cell marker for clonal analysis of development of the extraembryonic endoderm in the mouse. *J. Embryol. exp. Morph.* **80**, 251–288.

GREIG-SMITH, P. (1983). *Quantitative Plant Ecology*. Oxford: Blackwell.

HAUENSCHILD, C. C. (1980). Growth control of endothelial cells in atherogenesis and tumor angiogenesis. *Adv. Microcirc.* **9**, 226–251.

JENKINSON, J. W. (1925). *Vertebrate Embryology. The Early History of the Embryo*. London: Humphrey Milford (for Oxford University Press).

LEWIS, J. H., SUMMERBELL, D. & WOLPERT, L. (1972). Chimaeras and cell lineage in development. *Nature, Lond.* **239**, 276–278.

LINDLEY, D. V. & SCOTT, W. F. (1984). *New Cambridge Elementary Statistical Tables*. Cambridge: Cambridge University Press.

MCLAREN, A. (1976). *Mammalian Chimaeras*. Cambridge: Cambridge University Press.

MINTZ, B. (1971*a*). Allophenic mice of multi-embryo origin. In *Methods in Mammalian Embryology* (ed. J. Daniel), pp. 186–214. San Francisco: Freeman.

MINTZ, B. (1971*b*). Clonal basis of mammalian differentiation. In *Control Mechanisms of Growth and Differentiation. Symp. Soc. exp. Biol.* **25** (ed. D. D. Davis & M. Balls), pp. 345–370. Cambridge: Cambridge University Press.

MULLEN, R. J. (1977). Site of *pcd* gene action and Purkinje cell mosaicism in cerebellar of chimaeric mice. *Nature, Lond.* **270**, 245–247.

PONDER, B. A. J. & WILKINSON, M. M. (1983). Organ-related differences in binding of *Dolichos biflorus* agglutinin to vascular endothelium. *Devl Biol.* **98**, 535–541.

PONDER, B. A. J., FESTING, M. F. & WILKINSON, M. M. (1985*a*). An allelic difference determines reciprocal patterns of expression of binding sites for *Dolichos biflorus* lectin in inbred strains of mice. *J. Embryol. exp. Morph.* **87**, 229–239.

PONDER, B. A. J., SCHMIDT, G. H., WILKINSON, M. M., WOOD, M. J., MONK, M. & REID, A. (1985*b*). Derivation of mouse intestinal crypts from single progenitor cells. *Nature, Lond.* **313**, 689–691.

POOL, J. C. F., SANDERS, A. G. & FLOREY, H. W. (1958). The regeneration of aortic endothelium. *J. Path. Bac.* **75**, 133–139.

ROSS, G. J. S. (1980). *MLP (Maximum Likelihood Program)*. Harpenden: Rothamstead Experimental Station.

SCHMIDT, G. H., GARBUTT, D. J., WILKINSON, M. M. & PONDER, B. A. J. (1985*a*). Clonal analysis of intestinal crypt populations in mouse aggregation chimaeras. *J. Embryol. exp. Morph.* **85**, 121–130.

SCHMIDT, G. H., WILKINSON, M. M. & PONDER, B. A. J. (1984). A method for the preparation of large intact sheets of intestinal mucosa: application to the study of mouse aggregation chimaeras. *Anat. Rec.* **210**, 407–411.

SCHMIDT, G. H., WILKINSON, M. M. & PONDER, B. A. J. (1985*b*). Cell migration pathway in the intestinal epithelium: an *in situ* marker system using mouse aggregation chimaeras. *Cell* **40**, 425–429.

SCHMIDT, G. H., WILKINSON, M. M. & PONDER, B. A. J. (1985*c*). Detection and characterisation of spatial pattern in chimaeric tissue. *J. Embryol. exp. Morph.* **88**, 219–230.

SCHMIDT, G. H., WILKINSON, M. M. & PONDER, B. A. J. (1986). Non-random spatial arrangement of clone sizes in chimaeric retinal pigment epithelium. *J. Embryol. exp. Morph.* **91**, 197–207.

SCHWARTZ, S. M. & BENDITT, E. P. (1973). Cell replication in the aortic endothelium: a new method for study of the problem. *Lab. Invest.* **28**, 699–707.

THORGEIRSSON, G. & ROBERTSON, A. L. (1978). The vascular endothelium – pathobiologic significance. A review. *Am. J. Pathol.* **93**, 803–848.

WEST, J. (1975). A theoretical approach to the relation between patch size and clone size in chimaeric mice. *J. theor. Biol.* **50**, 153–160.

WHITTEN, W. R. (1978). Combinatorial and computer analysis of random mosaics. In *Genetic Mosaics and Chimaeras in Mammals* (ed. L. B. Russell), pp 445–463. London: Plenum Press.

(Accepted 21 November 1985)